SECURITY C

AD-A234 599 DOCUMENTATION PAGE

DTIC ELECTE APR 22 1991 D

1a. REPORT Unclassified	1b. RESTRICTIVE MARKINGS
2a. SECURITY CLASSIFICATION AUTHORITY	3. DISTRIBUTION / AVAILABILITY OF REPORT
2b. DECLASSIFICATION / DOWNGRADING SCHEDULE	
4. PERFORMING ORGANIZATION REPORT NUMBER(S) Technical Report No. 27	5. MONITORING ORGANIZATION REPORT NUMBER(S)
6a. NAME OF PERFORMING ORGANIZATION The University of Texas at Arlington / 6b. OFFICE SYMBOL (If applicable)	7a. NAME OF MONITORING ORGANIZATION Office of Naval Research
6c. ADDRESS (City, State, and ZIP Code) Center for Advanced Polymer Research Department of Chemistry, Box 19065, University of Texas at Arlington, Arlington, TX. 76019	7b. ADDRESS (City, State, and ZIP Code) 800 North Quincy Street Arlington, Virginia 22217
8a. NAME OF FUNDING / SPONSORING ORGANIZATION Defense Advanced Research Projects Agency / 8b. OFFICE SYMBOL (If applicable) DARPA	9. PROCUREMENT INSTRUMENT IDENTIFICATION NUMBER N00014-90-J-1320
8c. ADDRESS (City, State, and ZIP Code) 1410 Wilson Boulevard Arlington, Virginia 22209	10. SOURCE OF FUNDING NUMBERS: PROGRAM ELEMENT NO. / PROJECT NO. / TASK NO. / WORK UNIT ACCESSION NO.

11. TITLE (Include Security Classification)
Electrochemically Induced Charge and Mass Transport in Polypyrrole/Poly(styrene sulfonate) Molecular Composites

12. PERSONAL AUTHOR(S)
Charles K. Baker, Yong-Jian Qiu and John R. Reynolds

13a. TYPE OF REPORT	13b. TIME COVERED	14. DATE OF REPORT (Year, Month, Day)	15. PAGE COUNT
Technical	FROM _____ TO _____	April 12, 1991	36

16. SUPPLEMENTARY NOTATION
Paper in press in J. Phys. Chem.

17. COSATI CODES			18. SUBJECT TERMS (Continue on reverse if necessary and identify by block number)
FIELD	GROUP	SUB-GROUP	Polypyrrole; poly(styrene sulfonate); composites; quartz crystal microbalance; diffusion constants

19. ABSTRACT (Continue on reverse if necessary and identify by block number)

Polypyrrole/poly(styrene sulfonate) (PP/PSS) molecular composites have been synthesized by the electrochemical polymerization of pyrrole in the presence of sodium poly(styrene sulfonate) (PSS^-Na^+). Their synthesis and charge transport properties have been investigated by a combination of electrochemical and gravimetric techniques using the Electrochemical Quartz Crystal Microbalance (EQCM). Electropolymerization in water at 0.8 V vs. Ag/AgCl yields a partially hydrated polymer complex with sulfonate dopant anions from the PSS. Mass transport is found to be cation specific, as expected for a composite system, with the polyelectrolyte chains physically entrapped within the polymer membrane. Frequency responses of the EQCM during electrochemical switching are found to increase with increasing electrolyte cation mass as $Li^+ \cong Na^+ < Cs^+ < Et_4N^+ < Bu_4N^+$. Chronogravimetric and chronocoulometric analyses of PP/PSS^-Na^+ yield apparent diffusion constants, D_{app}, between 10^{-9} and 10^{-11} $cm^2\ s^{-1}$ for mobile hydrated Na^+ species. Though the determination of theses values are complicated by the exact determination of the concentration of electroactive sites (C_o^*), it is evident that reductive transport processes are faster than oxidative transport processes during switching.

20. DISTRIBUTION / AVAILABILITY OF ABSTRACT	21. ABSTRACT SECURITY CLASSIFICATION
☒ UNCLASSIFIED/UNLIMITED ☐ SAME AS RPT. ☐ DTIC USERS	Unclassified
22a. NAME OF RESPONSIBLE INDIVIDUAL Dr. JoAnn Milliken	22b. TELEPHONE (Include Area Code) (202) 696-4410 / 22c. OFFICE SYMBOL

DD FORM 1473, 84 MAR — 83 APR edition may be used until exhausted. All other editions are obsolete. SECURITY CLASSIFICATION OF THIS PAGE

DEFENSE ADVANCED RESEARCH PROJECTS AGENCY/OFFICE OF NAVAL RESEARCH

Grant N00014-90-J-1320

R&T Code a400008df307

Technical Report No. 27

Electrochemically Induced Charge and Mass Transport in Polypyrrole/ Poly(styrene sulfonate) Molecular Composites

by

Charles K. Baker
Yong-Jian Qiu
John R. Reynolds

Center for Advanced Polymer Research
Department of Chemistry
Box 19065
The University of Texas at Arlington
Arlington, Texas 76019-0065

April 12, 1991

A-1

J. Phys. Chem.

Electrochemically Induced Charge and Mass Transport in Polypyrrole/Poly(styrene sulfonate) Molecular Composites

Charles K. Baker,[1] Yong-Jian Qiu and John R. Reynolds*

Contribution from the
Center for Advanced Polymer Research
Department of Chemistry, The University of Texas at Arlington
Arlington, Texas 76019-0065

Abstract: Polypyrrole/poly(styrene sulfonate) (PP/PSS) molecular composites have been synthesized by the electrochemical polymerization of pyrrole in the presence of sodium poly(styrene sulfonate) (PSS^-Na^+). Their synthesis and charge transport properties have been investigated by a combination of electrochemical and gravimetric techniques using the Electrochemical Quartz Crystal Microbalance (EQCM). Electropolymerization in water at 0.8 V vs. Ag/AgCl yields a partially hydrated polymer complex with sulfonate dopant anions from the PSS. Mass transport is found to be cation specific, as expected for a composite system, with the polyelectrolyte chains physically entrapped within the polymer membrane. Frequency responses of the EQCM during electrochemical switching are found to increase with increasing electrolyte cation mass as $Li^+ \equiv Na^+ < Cs^+ < Et_4N^+ < Bu_4N^+$. Chronogravimetric and chronocoulometric analyses of PP/PSS^-Na^+ yield apparent diffusion constants, D_{app}, between 10^{-9} and 10^{-11} $cm^2\ s^{-1}$ for mobile hydrated Na^+ species. Though the determination of theses values are complicated by the exact determination of the concentration of electroactive sites (C_o^*), it is evident that reductive transport processes are faster than oxidative transport processes during switching.

Introduction

The electrochemical preparation of electrically conductive blends and composites of polyheterocycles, with a variety of carrier polymers has led to a new class of multicomponent materials with controllable electrical, electrochemical and mechanical properties. The ultimate properties result from the intrinsic properties of both the polyheterocycle, and the carrier polymer, along with specific interactions between the two polymers. A number of composites of polyheterocycles with matrix supporting polymers and polyelectrolytes have appeared in the literature. Early work on these systems involved the electrochemical polymerization of a heterocycle within a predeposited, solvent swollen thermoplastic polymer matrix on an electrode surface. Several systems have been prepared in this manner, including composites of polypyrrole with poly(vinyl chloride),[2] poly(vinyl alcohol),[3] polystyrene,[2c] poly(methyl methacrylate),[2c] and vinylidene chloride-vinyl chloride copolymers.[2c] This method has been improved by saturating the supporting polymer matrix with an electrolyte prior to deposition and subsequent electropolymerization.[4] A common problem encountered in films prepared by this method is an irregular conductivity across the thickness of the film as a result of the polymerization originating at the electrode/matrix interface which then proceeds outward through the film as the monomer diffuses in. These problems were only partially alleviated by the electrolyte doped host matrix.

Composite films of poly(3-methylthiophene) with poly(methyl methacrylate) and poly(vinyl chloride) have been prepared using a simple one-step procedure involving electropolymerization onto a metallic electrode from a solution containing 3-methylthiophene, supporting electrolyte, and the dissolved insulating polymer.[5] This technique allows for better control of the characteristics of the resulting materials and is able to produce composite films with spatially homogeneous conductivity and a good electrochemical response. Polypyrrole/poly-electrolyte composites employing a multicomponent system, consisting of PTFE membrane (Gore-tex) having a porous structure coated with a perfluorosulfonate ionomer (Nafion), as the host polymer matrix have been investigated.[6]

A final type of composite system can be prepared by the electrochemical polymerization of a heterocycle in the presence of a soluble anionic polyelectrolyte. This system offers an additional advantage in that the strengthening host material is also the dopant ion and is thus an intrinsic part of the conducting polymer composite matrix. The interactions between the positively charged polyheterocycle and charge compensating polyanion force intimate mixing of the two polymers; thus the material is a *molecular composite*. The initial work[7] in these molecular composites involved the polymerization of pyrrole in the presence of a number of polyanions. The support polymers were selected in an attempt to form elastic and melt processible conducting films.

Molecular composite films have also been electrochemically synthesized from methanol/acetonitrile solutions containing pyrrole and Nafion.[8] As above, the Nafion is serving as the supporting electrolyte and is thus incorporated as the dopant ion during conducting composite deposition. Comparison of these films, with films prepared by electropolymerization within precast Nafion matrices, showed that both methods yielded films with enhanced mechanical properties and retained their electroactivity by examination of the $Fe(CN)_6^{3-}$ and $Ru(NH_3)_6^{3+}$ redox systems. Electrochemical switching of PP/Nafion® was investigated[8b,c] and cation transport suggested. These measurements alone do not give a direct measure of the direction of ion flux during switching.

A number of other polyelectrolytes have been used in the direct electrodeposition of polypyrrole/polyelectrolyte molecular composites. These encompass a broad spectrum of sulfonated polymers including poly(vinyl sulfate),[9,10] poly(vinyl sulfonate),[10,12] poly(styrene sulfonate),[9-13] poly(styrene-co-maleic acid),[12] Stepantane A (sodium sulphonate of a naphthalene-formaldehyde polymer)[12] and poly(p-phenylenetere-phthalamide propane sulfonate).[14]

The believed cation specific mobility (called "pseudo-cathodic doping") of the poly(vinyl sulfate) composite system has been utilized to develop several novel applications. By combining the system with an anion exchangeable polypyrrole electrode (polypyrrole doped with a small anion) an electrochemical deionization system was constructed.[9,15] Another application developed with the poly(vinyl sulfate) composite utilizes the low redox couple potential, $E_{1/2}$ = -370 mV (vs.

S.C.E.), of this system relative to the free ion polypyrrole system, $E_{1/2}$ = +165 mV (vs. S.C.E.). By using the reduced polypyrrole/poly(vinyl sulfate) composite as the anode and the oxidized poly(pyrrole chloride) as the cathode, a P-P' type rechargeable battery was constructed.[16] Miller and Zhou[17] have used a composite of poly(N-methyl pyrrole) with poly(styrene sulfonate) as an electrically switchable cation exchanger but were not able to observe or control the ion transport rate.

Medium effects on electropolymerization have been investigated in the polypyrrole/poly-(styrene sulfonate) composite system via control of the electrical conductivity through variations in the polarity of the solvent in which the films were prepared.[13] By addition of 1,4-dioxane to aqueous solutions of the sodium salt of poly(styrene sulfonate) and pyrrole, it was found that the resulting changes in polyelectrolyte conformation caused changes in the electrical conductivity of the resulting film. More highly extended polyelectrolyte conformations, obtained in aqueous solutions, led to higher electrical conductivity.

Charge-transport rates in polyheterocycles, in general, are believed to be controlled by ion diffusion/migration into and out of the polymer membrane.[18-21] In the polyheterocycle/poly-electrolyte molecular composites, the polymeric dopant anions are expected to be entrapped and immobile forcing the electrolyte cation to be the mobile species. This situation is also created when the dopant anion is covalently attached (i.e., bound) to the polyheterocycle backbone. In these "self-doped" polyheterocycles,[22-24] cation specific transport has been monitored microgravimetrically,[23b] via pH changes at the polymer/electrolyte interface[25] and with X-ray microprobe analysis.[25]

In this paper we report on the electrochemical preparation and ion transport during electrochemical switching of the molecular composite of polypyrrole synthesized with poly(sodium 4-styrene sulfonate) (PP/PSS). We have utilized the electrochemical quartz crystal microbalance (EQCM) in solution for the first time to directly measure polypyrrole composite deposition during synthesis and investigate the ion transport as mass fluxes in detail during switching. A preliminary note appeared after we had completed this work that briefly addressed the gravimetric changes in

PP/PSS during switching.[26] The direction of these mass fluxes, and their relative rates, are important parameters in determining polymer:solvent:ion interactions and the applicability of these materials as useful electrodes.

The EQCM has recently been developed as an extremely versatile technique for monitoring gravimetric changes occurring at an electrode surface. It has been applied to studies of metal, semiconductor and metal oxide surfaces,[27] redox polymers,[28] electrodepositable dyes[29] and electrically conducting polymers.[30] In only one instance,[30d] outside of the present study, has the EQCM been used to examine an electrically conducting polymer composite material. This material was prepared by the electropolymerization of aniline within pre-cast films of Nafion, as opposed to the direct electropolymerization/deposition technique described here for polypyrrole/poly(styrene sulfonate).

Experimental Section

Pyrrole (Aldrich Chemicals) was purified immediately before use by passing it through a microcolumn constructed from a Pasteur pipet, glass wool and activated alumina. This procedure was repeated several times until a colorless liquid was obtained. Common electrolytes were used as received. The Na^+ salt of poly(styrene sulfonate) (PSS^-Na^+) (molecular weight = 100,000, 100% sulfonated) was purchased from Aldrich Chemicals. The water used in these experiments was deionized and distilled using a Corning Mega-Pure distillation system. All electrolyte/ monomer solutions were purged with either nitrogen or argon prior to use. Elemental analyses were performed by Galbraith Laboratories.

The EQCM is commonly used to determine mass changes at an electrode surface by monitoring changes in the resonant frequency (f) of an oscillating quartz crystal. Development of instrumentation which allows the EQCM to be operated under solution has led to a variety of systems[27-30] which have been studied using the technique. Details of the EQCM can be found in previous work.[30c] The frequency/mass relationship is described by the Sauerbrey equation[31] which can be written:

$$\Delta f = - \frac{2 f_o^2 \Delta M}{A \sqrt{\rho_q \mu_q}}$$

where f_o= resonant frequency of the unloaded quartz crystal sandwiched between two metallic electrodes, M = change in mass in grams, A = surface area of electrode or film, ρ_q = density of the quartz = 2.648 g cm^{-3}, μ_q = shear modules of quartz = 2.947 x 10^{11} dynes cm^{-2}. In these studies, we have employed an AT-cut quartz crystal (Inficon) which operates at 5 MHz in the thickness shear mode with a sensitivity of approximately 18 ng Hz^{-1} cm^{-2}. Opposing faces of the crystal were coated with gold keyhole-shaped electrodes. The crystal was mounted in an O-ring seal such that the area exposed to solution (~0.95 cm^2) was less than the area of oscillation (1.35 cm^2).

Results and Discussion

Polymerization and Deposition. The concurrent electropolymerization/deposition of polypyrrole/poly(styrene sulfonate) is illustrated in Figure 1 via an amperometric cyclic voltammogram (A-CV, solid line) and a corresponding gravimetric cyclic voltammogram (G-CV, dashed line) during the initial potential sweep from 0.0 to 1.1 V versus Ag/AgCl for an aqueous solution of 0.1 M pyrrole and 0.1 M PSS^-Na^+. The amperometric response exhibits an anodic peak potential, $E_{p,a}$, of 1.05 V and is typical for the oxidation and polymerization of pyrrole.[30c] The shape of this peak, and the lack of a corresponding cathodic peak on the reverse scan, is attributed to an irreversible electrochemical radical coupling reaction. The frequency response (dashed line) corresponds to the mass of polypyrrole/poly(styrene sulfonate) (PP/PSS), and some solvent, being deposited on the bare electrode surface. Examination of these results shows a concomitant initiation of current and polymer film deposition at approximately 0.6 V.

To examine the initial stages of polymerization, a potential step from 0.0 to 0.8 V was applied to an identical solution of pyrrole and poly(styrene sulfonate). This potential was selected because it gave fully developed current spikes and rising currents typical of the electrodeposition process.[30c] The resulting current and frequency responses were monitored at 50 ms intervals. This experiment was repeated 5 times, the results averaged, and are shown in Figure 2. A close

examination of these results indicates that the current spike is associated with a 5 Hz frequency increase followed by a rising current whose onset coincides with the deposition of polymer onto the electrode surface. This result is contrary to suggestions that the initial current spike is due to coverage of the electrode surface with a monolayer of polymer.[32] This observation is in agreement with ellipsometric data obtained, for the polymerization of thiophene, which suggested that the initial current spike may be due to the formation of solution intermediates (dimers → oligomers) which can accumulate in solution and eventually precipitate onto the electrode surface to form nucleation sites marked by the current transient minima.[33] The exact nature of the intermediates, and the conditions necessary for their participation in nucleation site formation, are still unclear.

The frequency decrease is linear as a function of time for a potential step from 0.0 to 0.8 V over a longer time interval which serves to indicate that the polymerization is not diffusion limited, but is controlled by the radical coupling reactions of oxidized species as observed in the electrochemical synthesis of poly(pyrrole tosylate).[30c] The frequency and charge vs. time data can be correlated by applying Faraday's Law to yield a relationship between charge vs. the number of moles of pyrrole deposited assuming an effective molecular weight of the depositing species. Stoichiometric ratios were determined by S:N elemental analyses carried out on PP/PSS films synthesized under identical conditions and effective molecular weight of 102 grams per mole of pyrrole deposited, as illustrated in Structure 1, was calculated. It should be noted that our analyses, showing a PSS^-/pyrrole ratio of 0.2, are identical to those reported previously.[9a,13]

Structure 1

The slope of the charge vs. moles pyrrole plot is proportional to n, the number of electrons per unit of pyrrole deposited. A slope proportional to 1.75 electrons per pyrrole was measured using 1000 data points with a correlation coefficient of .9999. This indicates a statistically linear relationship over the bulk of polymerization. The n-value of 1.75 is lower than the expected value of 2.2 which is based on 2 electrons required for formation of the polymer linkages and 0.2 electrons due

to the partial oxidation of the conjugated backbone.[30c] This low n-value indicates that more mass is being sensed by the QCM than expected for the measured amount of charge. There are two likely sources of this mass. For the possibility of solvent trapped in the film, we can assume both a high coulombic efficiency and complete stoichiometric usage of the sulfonate sites during polymerization. In a typical polymerization, a 3000 Hz change during film growth corresponds to a deposition of 5.04×10^{-5} grams on the electrode which separates out as 3.89×10^{-5} grams of polymer and 1.15×10^{-5} grams of solvent. This yields a ratio of approximately 2 solvent molecules per pyrrole unit in the chain.

For the possibility of incomplete stoichiometric usage of the sulfonate PSS^- sites as dopant ions, we can assume a high coulombic efficiency and the incorporation of very little solvent in the polymer matrix during polymerization. Again, assuming a frequency change of 3000 Hz, we would have a total mass change of 5.04×10^{-5} grams of which 3.89×10^{-5} grams are polymer and 1.15×10^{-5} grams are free (non-dopant) sodium styrene-sulfonate sites. This mass of free sodium styrenesulfonate sites corresponds to a 15 molar % excess, or a total PSS/pyrrole ratio of 0.35, which conflicts with elemental analysis of our films and that published by others.[9a,13]

The initial frequency changes, overall efficiency analysis, and cyclic voltammetric deposition experiments demonstrate two important factors about the polymerization of pyrrole in the presence of a polyelectrolyte. First, the polymerization mechanism is not affected, when compared to tosylate,[30c] by the use of the poly(styrene sulfonate) electrolyte/dopant system. Second, there is probably a combination of solvent incorporation and non-stoichiometric usage of sulfonate sites which results in a low observed n-value.

Films used to study the redox activity of the PP/PSS composite system were prepared by potentiostatic polymerization at 0.8 V from an aqueous solution of 0.1 M pyrrole and 0.1 M PSS^-Na^+. The thickness of these films was controlled by stopping the polymerization via opening the electrical circuit when the desired frequency response for deposition was obtained. This was done, as opposed to switching the potential to a value where polymerization ceases, in order to avoid electrochemical reduction of the as-made polymer film. The thickness was then calculated from the

density of the polymer (1.27 g cm^{-3}) and electrode surface area. An independent calibration of the film thickness was performed using a Tencor Instruments Alpha-Step 200 profilometer.

Our gravimetric method of determining film thickness offers several significant advantages. The first is the ability to estimate and control the thickness without having to remove and dry the film, thus exposing it to atmospheric contamination and possible destruction of the electroactive properties. The second is the ability to determine, in-situ, both the charge and mass for each film. This procedure provides a means of verifying the quality, and approximate doping level, of each film.

Ion Movement during the Initial Reduction. In the initial work on the electrochemical examination of the PP/PSS and other systems[12] an initial large peak was observed at approximately -0.7 V vs. SCE during the *initial* cathodic CV sweep in a monomer free solution. This feature was not observed on subsequent scans, but was replaced by a lower current reproducible reduction peak, at slightly higher potentials (-0.5 V vs. SCE). It was concluded that the initial cathodic process was accompanied by a shrinkage of the polymer film and, in the case of small dopant ions, expulsion of the anion.

In our study of this initial reduction process, PP/PSS composite films were rinsed thoroughly with water and returned to a monomer free 0.1 M aqueous solution of PSS^-Na^+. The films in the oxidized state were then stepped from the potential value at which the film was synthesized (0.8 V) to a potential value to fully reduce the film (-1.0 V). These experiments were repeated for film thicknesses ranging from 140 to 1400 nanometers. Large frequency decreases (mass gains) ranging from 700 to 2500 Hz were observed independent of film thickness. This observed frequency response range corresponds to a mass increase much larger than would be expected if all of the sulfonate sites in the neutral polymer matrix were being compensated by free Na^+ ions from the supporting electrolyte solution. For instance, the maximum expected frequency change during the reduction of 5.04 x 10^{-5} grams of PP/PSS (3000 Hz during polymerization or *ca.* 420 nm) would be 135 Hz (2.27 x 10^{-6} grams of Na^+ ions). This assumes a dopant level of approximately 20% and that the sodium atoms enter the film unsolvated. Large frequency

decreases are also observed during the first cathodic cyclic voltammetric sweep. Although the CV is not shown here, it confirms the presence of an anomalous peak at -0.7 V seen by other researchers [12] and correlates with the large mass increase found in our potential step experiments. In that the only mobile ionic species in this system are the Na^+ ions, as detailed below, a significant amount of water is penetrating into the film at this time also. The fact that the observed frequency change is independent of film thickness is probably due to extremely subtle variances in the handling of the films during rinsing.

Despite the inconsistent magnitude of the frequency response, the *time* that was needed to fully insert all of the Na^+ (and solvent molecules) into the polymer films was dependent on film thickness. If we compare the mass of Na^+ ions inserted into the film during this process with what would be expected, assuming 100% of the sulfonate groups are being compensated, we find that there are approximately 3-19 H_2O molecules per Na^+ ion being inserted independent of film thickness. These results suggest that subtle differences in polymerization conditions and polymer film handling can greatly affect the ultimate degree of solvation in a film. The general observation that the electrochemistry of electroactive polyheterocycle films requires a "break in" period, and actually improves with repeated cycling, can now be explained. The source of the improved electrochemistry lies in the necessity that solvent be present within the polymer matrix in order for ions to move freely into and out of the film during redox cycling. The fact that the degree of solvation appears to vary widely with little effect on the electroactivity suggests that once a film reaches a critical level of solvation, further solvation has little effect on change transport properties.

Nature of the Mobile Species. Confirmation that the mobile species are cations has been accomplished by comparing the amperomeric (A-CV) and gravimetric (G-CV) response of *ca.* 420 nm (3000 Hz during synthesis) PP/PSS film in three different sodium electrolytes. Figure 3 shows that the A-CV and G-CV responses observed for PP/PSS in NaCl, $NaClO_4$ and PSS^-Na^+ is independent of electrolyte type. This is as expected under conditions in which both Na^+ and water are mobile during switching. The observed 30 to 60 Hz frequency difference between the beginning and the end of the scan is likely due to slow recovery of water into the film.

Examination of the *absolute* microbalance frequency on consecutive scans shows that the microbalance equilibrates towards its original frequency between scans when held at -1.0 V.

Changing the cation of the electrolyte system has a profound effect on both the amperometric and gravimetric responses of the PP/PSS during switching. All of the alkali metal ions give A-CV responses that are quite similar, as shown in Figure 4a. The tetraalkylammonium ions, on the other hand, require significantly higher potentials to oxidize the film. This is shown for tetraethylammonium (Et_4N^+) ($E_{p,a}$ = -0.05 V) and tetrabutylammonium (Bu_4N^+) ($E_{p,a}$ = +0.15 V). The shifting of the peak potential in these dynamic experiments can be attributed to the mobility of the ions in the polymer membrane. This mobility can be affected by a variety of variables which include film resistance, ion pairing and, possibly most important, ionic volume. The fact that there is a significant difference in $E_{p,a}$ when using Et_4N^+ and Bu_4N^+, and that there is little difference seen in the hydrated alkali metal ions, suggests that the most important parameter is the volume within the membrane required for ion transport.

The gravimetric responses are also a strong function of the *mass* of the mobile species. Figure 4b shows the G-CV for PP/PSS using Li^+, Na^+, Cs^+, Et_4N^+ and Bu_4N^+. The much higher frequency responses for the higher mass ions show that the cations are undoubtedly the mobile species during switching. The driving force for this movement is the necessity that the positive charge created on the polypyrrole backbone, through the removal of π-electrons, be stabilized by the styrenesulfonate anions. This results in the ionic disassociation of the cation with the sulfonate groups upon oxiation, thus forcing the cations to leave the film in order to achieve charge neutrality. Upon any subsequent reduction, there is a mass increase associated with a movement of cations back into the film in order to compensate the charge associated with the anionic styrene sulfonate sites which are no longer serving as dopant ions.

Chronogravimetry and Chronocoulometry. In addition to the nature of the mobile species and its relative mass, the EQCM technique allows us to examine charge transport rates by monitoring mass fluxes via frequency changes. PP/PSS composites were prepared, as described

above, rinsed thoroughly with water to remove any excess monomer, and subsequently placed in a monomer free aqueous solution of PSS^-Na^+. The films were then equilibrated at a rest potential (-1.0 V) and subsequently stepped from this rest potential to an oxidative potential of -0.25 V and subsequently returned.

The charge and frequency vs. time responses for a typical experiment for four consecutive potential steps are shown in Figures 5a and 5b. The similar shape of these responses serves to demonstrate the analogous and complementary information which can be obtained from the chronocoulometric and chronogravimetric data as well as the relationship between the transport of charge and movement of ions in electroactive conducting polymers. The fact that the current does not limit during oxidation over this time scale, while the frequency response does, may be attributed to the non-faradaic nature of capacitive charging. The frequency vs. time response, Figure 5b, shows that upon oxidation there is a mass decrease corresponding to the movement, or diffusion and migration of Na^+ ions out of the polymer film, in agreement with our scanning experiments. The magnitude of this frequency response, 110 Hz for a 3000 Hz (420 nm) film during deposition, represents the movement of approximately 1.85×10^{-6} grams. If we make the assumption that the Na^+ ions leave the film unsolvated (which is of course unlikely) then 8.0×10^{-8} moles of Na^+ are mobile and the apparent active dopant level is 16%. Since solvent flux is necessary,[34] the actual amount of charge compensation occurring in the time frame of this experiment is significantly lower than possible in a 20 mol % doped film. This is most likely due to the electrochemical inaccessibility of a significant portion of the charged sites in the polypyrrole film. This electrochemical switching has been repeated up to 20 redox cycles showing reproducible frequency shifts.

To characterize the relative mass and charge transport rates of these films from the chronogravimetric and chronocoulometric data, charge and frequency results were plotted versus $t^{1/2}$. From the slope of these plots, and the integrated Cottrell equations for both charge and mass, apparent charge transport constants (D_{app}) were calculated. It should be noted that this method only yields comparative values for ion transport rates. The fact that the polymer is changing from

an insulator to a conductor makes absolute quantitative analysis difficult,[21] but the results lend insight into the relative transport rates as a function of film thickness and redox process.

Figures 6 and 7 show the charge vs. $t^{1/2}$ data for the first 3.5 seconds during the reductive and oxidative potential steps, respectively. This was done for films with thicknesses ranging from 140 nm to 1400 nm. The linear portion on these figures corresponds to the time regime in which semi-infinite diffusion behavior occurs and were used to calculate D_{app}. Figure 6 shows the results for the reductive process in which the Na^+ ions are moving into the composite film. The length of the semi-infinite time regime is evident as a break in the increase of Q with $t^{1/2}$ and is dependent on the thickness of the film. After determination of D_{app} (see below), the length of this semi-infinite diffusion behavior corresponds well with the length of time ($\sqrt{2\ Dt}$) it is expected to take a Na^+ ion, from outside the film, to reach the boundary represented by the supporting metallic electrode. Figure 7 shows the results for the oxidation process in which the Na^+ ions are moving out of the composite film. The length of the semi-infinite time regime is not as evident as during reduction.

Figure 8 shows the frequency vs. $t^{1/2}$ relationship during the reductive process in which Na^+ ions are moving into the polymer film. The magnitude of the mass change shows a moderate correlation with film thickness and the length of semi-infinite diffusion behavior is clearly marked. Comparison of Figure 8 with the simultaneously measured charge vs. $t^{1/2}$ data seen in Figure 6 serves to illustrate the correlation between the movement of charge and mass in these films. The break points in these curves occur at approximately the same time as expected if charge transport is controlled by ion mobility.

Figure 9 shows the frequency vs. $t^{1/2}$ relationship during the oxidative process in which sodium ions are moving out of the polymer composite. The magnitude of the frequency change shows little correlation with film thickness and the semi-infinite time regime is not clear, as expected from the results of Figure 7.

To calculate the D_{app} values via the integrated Cottrell equation, C_o^* (the concentration of redox sites) must be known. This was done using the method of Nagasubramanian et al.[8b] where this value can be determined from the total charge (Q_f) passed:

$$Q_f = LFAC_o^*$$

where L = film thickness and A = area. Here, we have measured Q_f directly coulometrically and utilized microbalance frequency changes, with an assumed effective mass per charge, to determine the number of accessible redox sites in each experiment. Once C_o^* is known, the slopes of the charge and frequency vs. $t^{1/2}$ plots shown in Figures 6-9 were determined for the data contained in the semi-infinite diffusion time regimes. Determination of this time regime was simple for the reductive processes with distinct breaks and more complicated for the oxidation process. In the latter, statistical methods were used to select the best break point between the semi-infinite and infinite time regimes.

Using the initial slopes ($D_{app}^{1/2} C_o^*$) from the results in Figures 6-9, the D_{app} values were determined and are shown in Table 1. Several important trends can be seen in this data. The first is that both charge and mass are generally transported at a higher rate during the reductive process as compared to the oxidative process. The origin of this effect has several possible sources. The most obvious lies in the fact that, during the initial stages of the reduction process, the film is electrically conducting and thus can easily support charge transport. Another possibility is the ionic concentration gradient set-up during reduction is greater than that during oxidation. A high ion content in both the film and electrolyte would result in a reduction of the ion mobility, and thus charge transport rate, during the oxidative process. This can be contrasted to the reduction process (starting with the oxidized form of the polymer) in which the free cations in solution are able to freely diffuse back into the cation starved film to compensate the charge of the immobilized anions.

The second important trend seen in this data is that the concentration of accessible redox sites decreases with increasing film thickness. This trend in our data may result from thin films having either (or both): 1) fewer defects along the polymer chain which results in a greater mean conjugation length or, 2) a larger degree of interchain order within the polymer film and thus a

more dense, and possibly semi-crystalline, morphology. These factors would result in a more efficient use of existing redox sites in thin films and thus a higher observable redox site concentration. However, as the film gets thicker the number of conjugation defects increases and the morphology of the polymer becomes amorphous and more open. Both of these effects would lead to a decrease in the concentration of doped sites which can serve a redox centers and perhaps a lower doping level as the film gets thicker. Also accompanying this increase in defects and disorder will be a decrease in the conductivity of the film. While we have made no attempt to measure the conductivity of our films, the picture presented here corresponds nicely with work by Roncali et.al.[35] who have shown that the conductivity of thin films of poly(3-methylthiophene) is highly dependent on film thickness; also attributed to an increasing number of defects and a decrease in morphological order as the film gets thicker.

Also evident in Table 1 is that D_{app} is related to both the initial and final ion and redox site populations, along with ion transport kinetics. The fact that the decrease in concentration of accessible sites with film thickness causes an increase in the magnitude of D_{app}, does not necessarily mean the actual ion transport kinetics are becoming faster. The invariability of $D_{app}^{1/2} C_o^*$ with film thickness, and visual inspection of the initial slopes of Figures 6-9, demonstrate the initial charging and ion flux rates are independent of film thickness. This indicates that caution must be taken when attempting to obtain ion transport rate information by comparing D_{app} values.

Conclusions

The electropolymerization of pyrrole in aqueous PSS^-Na^+ solutions is a relatively efficient process with a measured 1.75 electrons/pyrrole required for polymer deposition. This difference from the expected value of 2.2 indicates that solvent is incorporated. A high fraction of the sulfonate sites on the polyanionic backbone are functioning as dopant ions. Though some may be included in the free ion form, elemental analysis results suggest efficient usage of the sulfonates. There is little correlation between the total mass uptake during the initial film reduction and film thickness with solvent to cation ratios ranging from 3 to 19. Cation-specific transport dominates

during electrochemical switching of the PP/PSS molecular composites in monomer free electrolyte with no tendency towards the incorporation of external anions. In addition, the electrochemical cycling from the reduced to oxidized states, and back, results in an incomplete mass recovery. This suggests that the transport of solvent is much slower and thus lags behind transport of ions. Gravimetric responses during switching are higher for heavier cations as expected. A comparison of the chronocoulometric and gravimetric responses show they correlate well, with the reduction process showing a sharper, more clearly marked semi-infinite time regime and a faster ion transport rate than the oxidation process. This latter behavior may be the result of two phenomena, the relatively high conductivity of the polymer initially and ion pairing. At the onset of reduction, the polymer film is able to support charge transport throughout, resulting in higher ion transport rates and a diffusion boundary marked by the supporting metallic electrode. At the onset of oxidation, the film is an insulator and therefore must first be oxidized at the interface with the supporting electrode. This releases the cations from their ionic interaction with the sulfonate groups allowing them to diffuse out through the neutral portion of the film into solution. During this diffusive process it is likely that the ions movement will be retarded through cooperative interactions with non-dopant sulfonate groups. This combination of effects would result in a relatively undefined boundary at the film/solution interface and a reduced ion transport rate.

Acknowledgement

This research was funded by the Defense Advanced Research Projects Agency, monitored by the Office of Naval Research. We appreciate the reviewers comments on charge transport and diffusion coefficients.

REFERENCES

1. Present address: Southwest Research Institute, San Antonio, Texas.
2. (a) Niwa, O.; Tamamura, T. *J. Chem. Soc., Chem. Commun.* **1984**, *817*. (b) DePaoli, M. A.; Waltman, R. J.; Diaz, A. F. *J. Chem. Soc., Chem. Commun.* **1984**, *1015*. (c) Niwa, O.; Hikita, M.: Tamamura, T. *Appl. Phys. Lett.* **1985**, *46*, 444.
3. Lindsey, S. E.; Street, G. B. *Synth. Met.* **1984**, *10*, 67.
4. Wang, T. T.; Tasaka, S.; Hutton, R. S.; Lu, P. Y. *J. Chem. Soc., Chem. Commun.* **1985**, 1343.
5. (a) Roncali, J. Garnier, F. *J. Phys. Chem.* **1988**, *92*, 833. (b) Roncali, J.; Garnier, F. *J. Chem. Soc., Chem. Commun.* **1986**, 783. (c) Roncali, J.; Master, A.; Garnier, F. *Synth. Met.* **1984**, *10*, 67.
6. Penner, R. M.; Martin, C. R. *J. Electrochem. Soc.* **1986**, *133*, 310.
7. Bates, N.; Cross, M.; Lines, R.; Walton, D. *J. Chem. Soc., Chem. Commun.* **1985**, 871.
8. (a) Fan, F. F.; Bard, A. J. *J. Electrochem. Soc.* **1986**, *133*, 301. (b) Nagasubramanian, G.; DiStefano, S.; Moacanin, J. *J. Phys. Chem.* **1986**, *90*, 4447. (c) Yoneyama, H.; Hirai, T.; Kuwabata, S.; Ikeda, O. *Chem. Lett.* **1986**, 1243.
9. (a) Shimidzu, T.; Ohtani, A.; Iyoda, T.; Honda, K. *J. Electroanal. Chem.* **1987**, *224*, 123. (b) Shimidzu, T.; Ohtani, A.; Honda, K. *J. Electroanal. Chem.* **1988**, *251*, 323.
10. Bidan, G.; Ehui, B.; Lapkowski, M. *J. Phys. D., Appl. Phys.* **1988**, *21*, 1043.
11. Noftle, R. E.; Pletcher, D. *J. Electroanal. Chem.* **1987**, *227*, 229.
12. Warren, L. F.; Anderson, D. A. *J. Electrochem. Soc.* **1987**, *134*, 101.
13. Glatzhofer, D. T.; Ulanski, J.; Wegner, G. *Polymer* **1987**, *28*, 449.
14. (a) Reynolds, J. R.; Baker, C. K.; Gieselman, M. B. *Amer. Chem. Soc., Div. Polym. Chem., Polym. Preprints* **1989**, *30*, 151. (b) Gieselman, M. B.; Reynolds, J. R. *Macromolecules*, **1990**, *23*, 3118.
15. Shimidzu, T.; Ohtani, A.; Iyoda, T.; Honda, K. *J. Chem. Soc., Chem. Commun.* **1986**, 1415.

16. Shimidzu, T.; Ohtani, A.; Iyoda, T.; Honda, K. *J. Chem. Soc., Chem. Commun.* **1987**, 327.

17. Miller, L. L.; Zhou, Q. X. *Macromolecules* **1987**, *20*, 1594.

18. (a) Burgmayer, P.; Murray, R. W. *J. Am. Chem. Soc.* **1982**, *104*, 6139. (b) Burgmayer, P.; Murray, R. W. *J. Phys. Chem.* **1984**, *88*, 2515.

19. Genies, E. M.; Pernaut, J. M. *Synth. Met.* **1984/85**, *10*, 117.

20. (a) Pickup, P. G.; Osteryoung, R. A. *J. Electroanal. Chem.* **1985**, *195*, 271. (b) Paulse, C. D.; Pickup, P. G. *J. Phys. Chem.* **1988**, *92*, 7002.

21. Penner, R. M.; Van Dyke, L. S.; Martin, C. R. *J. Phys. Chem.* **1988**, *92*, 5274.

22. (a) Patil, A. O.; Ikenoue, Y.; Wudl, F.; Heeger, A. J. *J. Am. Chem. Soc.* **1987**, *109*, 1858. (b) Patil, A. O.; Ikenoue, Y.; Basesca, N.; Colaneri, N.; Chen, J.; Wudl, F.; Heeger, A. J. *Synth. Met.* **1987**, *20*, 151.

23. (a) Sundaresan, N. S.; Basak, S.; Pomerantz, M.; Reynolds, J. R. *J. Chem. Soc., Chem. Commun.* **1987**, 621. (b) Reynolds, J. R.; Sundaresan, N. S.; Pomerantz, M.; Basak, S.; Baker, C. K. *J. Electroanal. Chem.* **1988**, *250*, 355.

24. Havinga, E. E.; van Horssen, L. W.; ten Hoeve, W.; Wynberg, H.; Meijer, E. W. *Polym. Bull.* **1987**, *18*, 277.

25. (a) Ikenoue, Y.; Chiang, J.; Patil, A. O.; Wudl, F.; Heeger, A. J. *J. Am. Chem. Soc.* **1988**, *110*, 2983. (b) Ikenoue, Y.; Uotani, N.; Patil, A. O.; Wudl, F.; Heeger, A. J. *Synth. Met.* **1989**, *30*, 305.

26. Naoi, K.; Lien, M. M.; Smyrl, W. H. *J. Electroanal. Chem.* **1989**, *272*, 273.

27. (a) Schumacher, R.; Borges, G.; Kanazawa, K. K. *Surf. Sci.* **1985**, *163*, L621. (b) Schumacher, R.; Gordon, J. G.; Melroy, O. *J. Electroanal. Chem.* **1987**, *216*, 127. (c) Grabbe, E. S.; Buck, R. P.; Melroy, D. *J. Electroanal. Chem.* **1987**, *223*, 67. (d) Deakin, M. R.; Melroy. O. *J. Electroanal. Chem.* **1988**, *239*, 321. (e) Deakin, M. R.; Li, T. T.; Melroy, O. *J. Electroanal. Chem.* **1988**, *243*, 343. (f) Mori, E.; Baker, C. K.; Reynolds,

J. R.; Rajeshwar, K. *J. Electroanal. Chem.* **1988**, *252*, 441. (g) Deakin, M. R.; Melroy, O, R. *J. Electrochem. Soc.* **1989**, *136*, 349.

28. (a) Ward, M. D. *J. Phys. Chem.* **1988**, *92*, 2049. (b) Bruckenstein, S.; Wilde, C. P.; Shay, M.; Hillman, A. R.; Loveday, D. C. *J. Electroanal. Chem.* **1989**, *258*, 457.
29. (a) Feldman, B. J.; Melroy, O. R. *J. Electroanal. Chem.* **1987**, *234*, 213. (b) Ostrom, G. S.; Buttry, D. A. *J. Electroanal. Chem.* **1988**, *256*, 411.
30. (a) Kaufman, J. H.; Kanazawa; K. K.; Street, G. B. *Phys. Rev. Lett.* **1984**, *53*, 2461. (b) Orata, D.; Buttry, D. A. *J. Am. Chem. Soc.* **1987**, *109*, 3574. (c) Baker, C. K.; Reynolds, J. R. *J. Electroanal. Chem.* **1988**, *251*, 307. (d) Orata, D.; Buttry, D. A. *J. Electroanal. Chem.* **1988**, *257*, 71.
31. Sauerbrey, G. *Z. Phys.* **1959**, *155*, 206.
32. Hillman, R. A.; Mallen, E. F. *J. Electroanal. Chem.* **1987**, *220*, 351.
33. Hamnett, A.; Hillman, A. R. *J. Electrochem. Soc.* **1988**, *135*, 2517.
34. Bruckenstein, S.; Hillman, A. R. *J. Phys. Chem.* **1988**, *92*, 4837.
35. (a) Roncali, J.; Yassar, A.; Garnier, F. *J. Chem. Soc., Chem. Commun.* **1988**, 581. (b) Roncali, J.; Yassar, A.; Garnier, F. *Macromolecules* **1989**, *22*, 804.

Table 1

Concentration of redox sites (C_o^*, M), chronocoulometric/chronogravimetric slopes ($D_{app}^{1/2} C_o^*$) and apparent diffusion constants (D_{app}, $cm^2 s^{-1}$) for PP/PSS composite films of different thickness

Film Thickness (nm)	Charge vs. $t^{1/2}$					
	Oxidation			Reduction		
	C_o^*	$D_{app}^{1/2} C_o^*$	D_{app}	C_o^*	$D_{app}^{1/2} C_o^*$	D_{app}
140	1.3×10^{-3}	8.7×10^{-9}	4.5×10^{-11}	2.3×10^{-3}	2.2×10^{-8}	9.2×10^{-11}
280	1.3×10^{-3}	1.7×10^{-8}	1.8×10^{-10}	1.7×10^{-3}	3.4×10^{-8}	3.9×10^{-10}
420	1.2×10^{-3}	1.9×10^{-8}	2.6×10^{-10}	1.4×10^{-3}	3.9×10^{-8}	7.6×10^{-10}
700	1.2×10^{-3}	2.6×10^{-8}	4.7×10^{-10}	1.3×10^{-3}	5.5×10^{-8}	1.8×10^{-9}
1400	9.3×10^{-4}	2.9×10^{-8}	9.8×10^{-10}	9.9×10^{-4}	6.2×10^{-8}	3.9×10^{-9}

Film Thickness (nm)	Frequency vs. $t^{1/2}$					
	Oxidation			Reduction		
	C_o^*	$D_{app}^{1/2} C_o^*$	D_{app}	C_o^*	$D_{app}^{1/2} C_o^*$	D_{app}
140	5.7×10^{-3}	4.1×10^{-8}	5.2×10^{-11}	5.7×10^{-3}	4.7×10^{-8}	6.8×10^{-11}
280	---	---	---	---	---	---
420	3.3×10^{-3}	3.6×10^{-8}	1.2×10^{-10}	4.1×10^{-3}	5.5×10^{-8}	1.8×10^{-10}
700	3.1×10^{-3}	4.2×10^{-8}	1.8×10^{-10}	3.1×10^{-3}	6.0×10^{-8}	3.7×10^{-10}
1400	3.5×10^{-3}	3.8×10^{-8}	1.2×10^{-10}	---	---	---

FIGURE CAPTIONS

Figure 1. Simultaneously measured amperometric (solid) and gravimetric cyclic voltammograms (dashed) of a PP/PSS composite film obtained in an aqueous solution of 0.1 M PSS^-Na^+. Scan rate = 25 mV/sec.

Figure 2. Chronoamperometric and chronogravimetric responses obtained during the initial current spike for a constant potential polymerization of pyrrole from an aqueous solution of 0.1 M PSS^-Na^+.

Figure 3. Amperometric and gravimetric cyclic voltammograms of PP/PSS in (1) 0.1 M NaCl, (2) 0.1 M $NaClO_4$, (3) 0.1 M NaPSS

Figure 4. (a) Amperometric cyclic voltammograms of PP/PSS in (1) 0.1 M LiCl, (2) 0.1 M CsCl, (3) 0.1 M Et_4NCl, (4) 0.1 M Bu_4NCl, (5) 0.1 M NaPSS; (b) gravimetric cyclic voltammograms of PP/PSS in (1) 0.1 M LiCl, (2) 0.1 M CsCl, (3) 0.1 M Et_4NCl, (4) 0.1 M Bu_4NCl, (5) 0.1 M NaPSS.

Figure 5. (a) Chronocoulometric response of a 420 nm thick PP/PSS film during four successive oxidation and reduction steps in an aqueous solution of 0.1 M PSS^-Na^+. (b) Chronogravimetric response of a 420 nm thick PP/PSS film during four succes-sive oxidation and reduction steps in an aqueous solution of 0.1 M PSS^-Na^+.

Figure 6. Charge vs. $t^{1/2}$ during the reduction of several PP/PSS films of various thicknesses in an aqueous solution of 0.1 M PSS^-Na^+, (a) 140 nm, (b) 280 nm, (c) 420 nm, (d) 700 nm, (e) 1400 nm. The initial linear portion corresponds to the time of semi-infinite diffusion behavior.

Figure 7. Charge vs. $t^{1/2}$ during the oxidation of several PP/PSS^- films of various thicknesses in an aqueous solution of 0.1 M PSS^-Na^+, (a) 140 nm, (b) 280 nm, (c) 420 nm, (d) 700 nm, (e) 1400 nm. The initial linear portion corresponds to the time of semi-infinite diffusion behavior.

Figure 8. Frequency change vs. $t^{1/2}$ for the reduction of PP/PSS films of various thicknesses measured simultaneously with Figure 7 during the semi-infinite diffusion time regime, (a) 140 nm, (b) 420 nm, (c) 1400 nm.

Figure 9. Frequency change vs. $t^{1/2}$ for the oxidation of PP/PSS films of various thicknesses measured simultaneously with Figure 7 during the semi-infinite diffusion time regime, (a) 420 nm, (b) 700 nm, (c) 1400 nm.

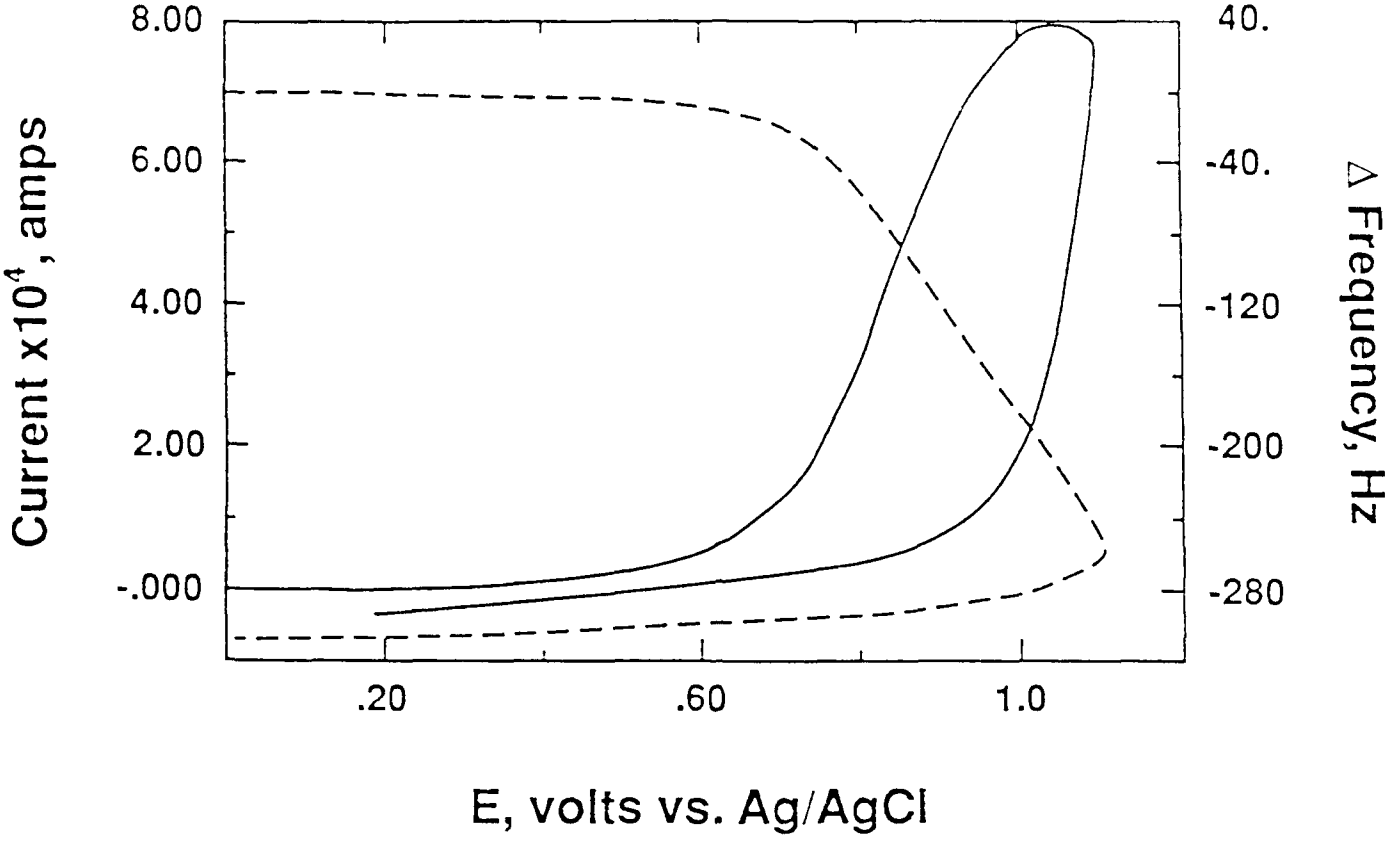
8.00
6.00
4.00
2.00
-.000
Current x10^4, amps
40.
-40.
-120
-200
-280
Δ Frequency, Hz
.20
.60
1.0
E, volts vs. Ag/AgCl

F2

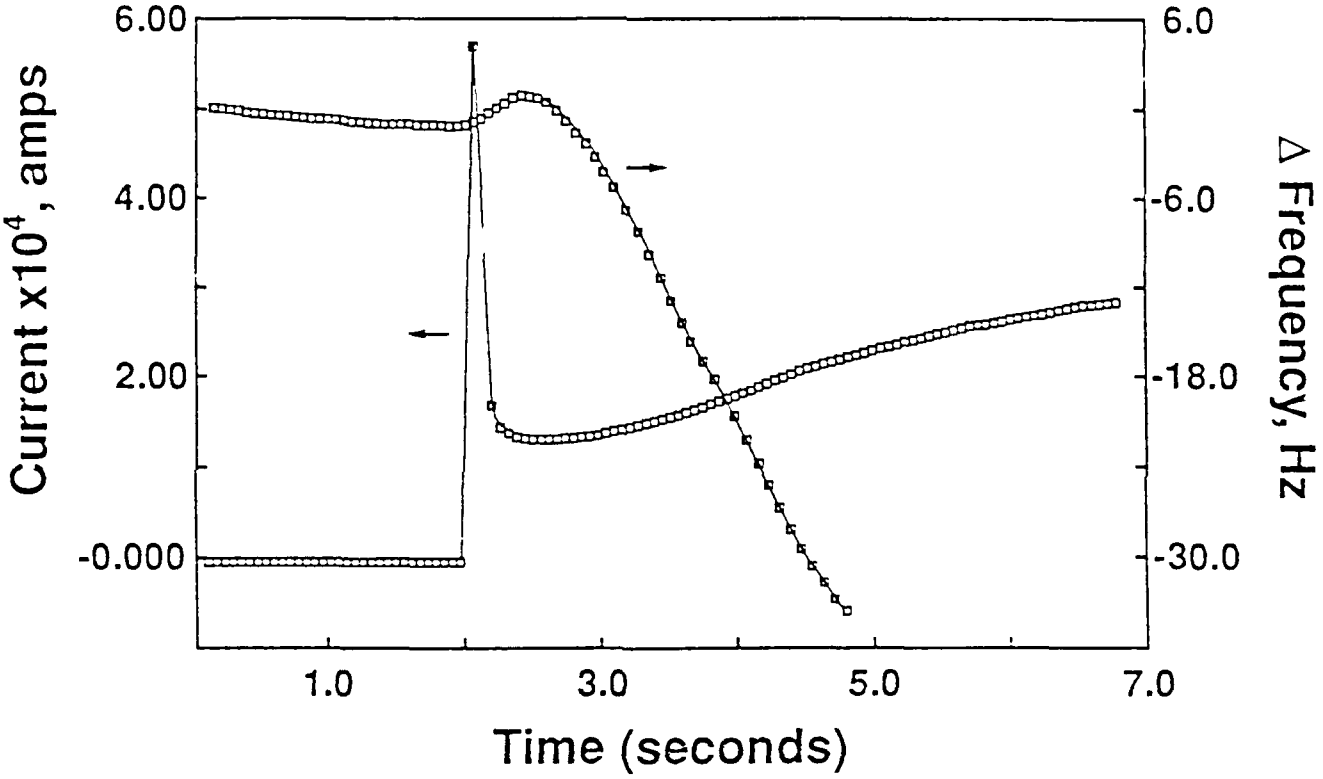
6.00
4.00
2.00
-0.000
Current x10^4, amps
6.0
-6.0
-18.0
-30.0
Δ Frequency, Hz
1.0
3.0
5.0
7.0
Time (seconds)

F 3

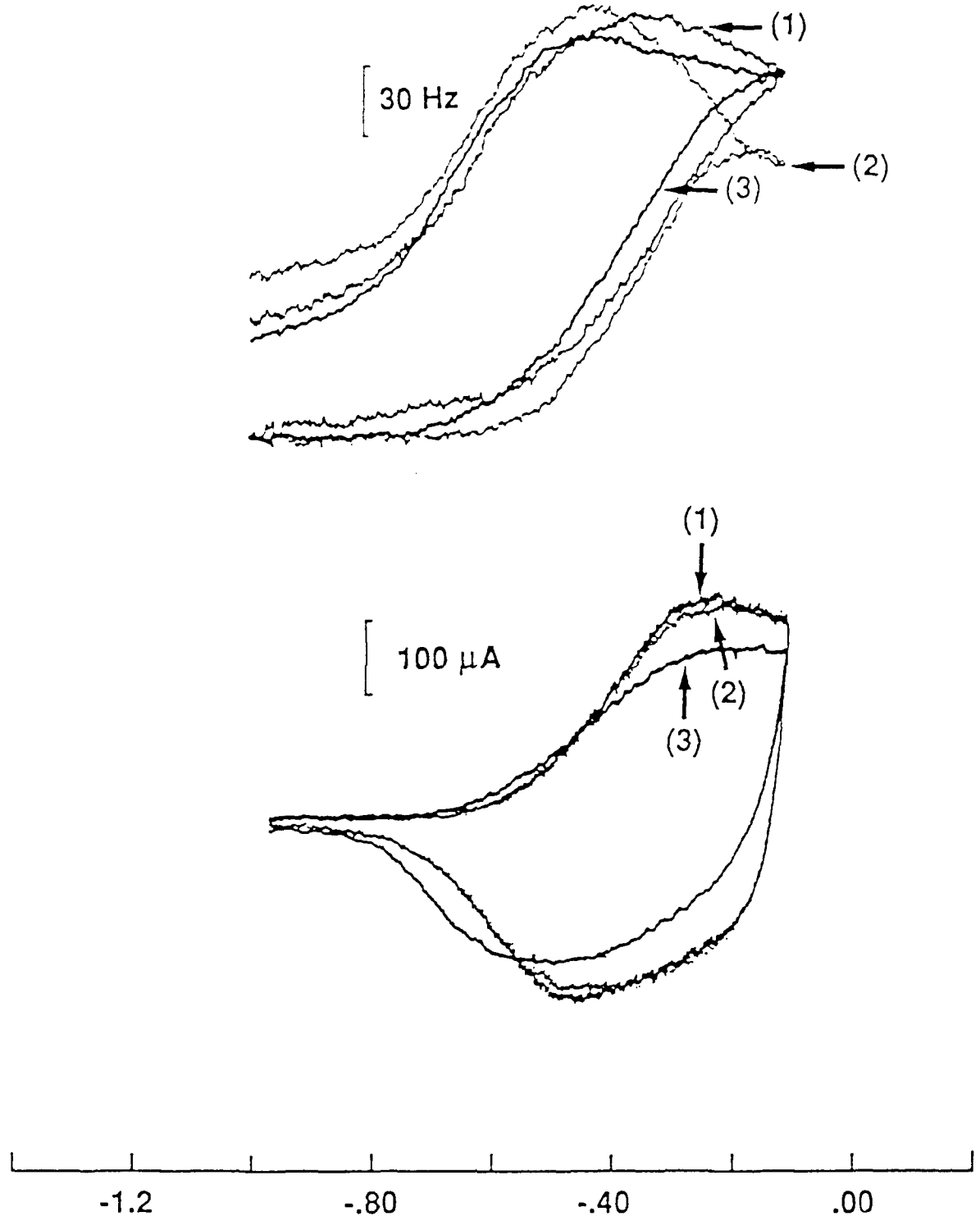

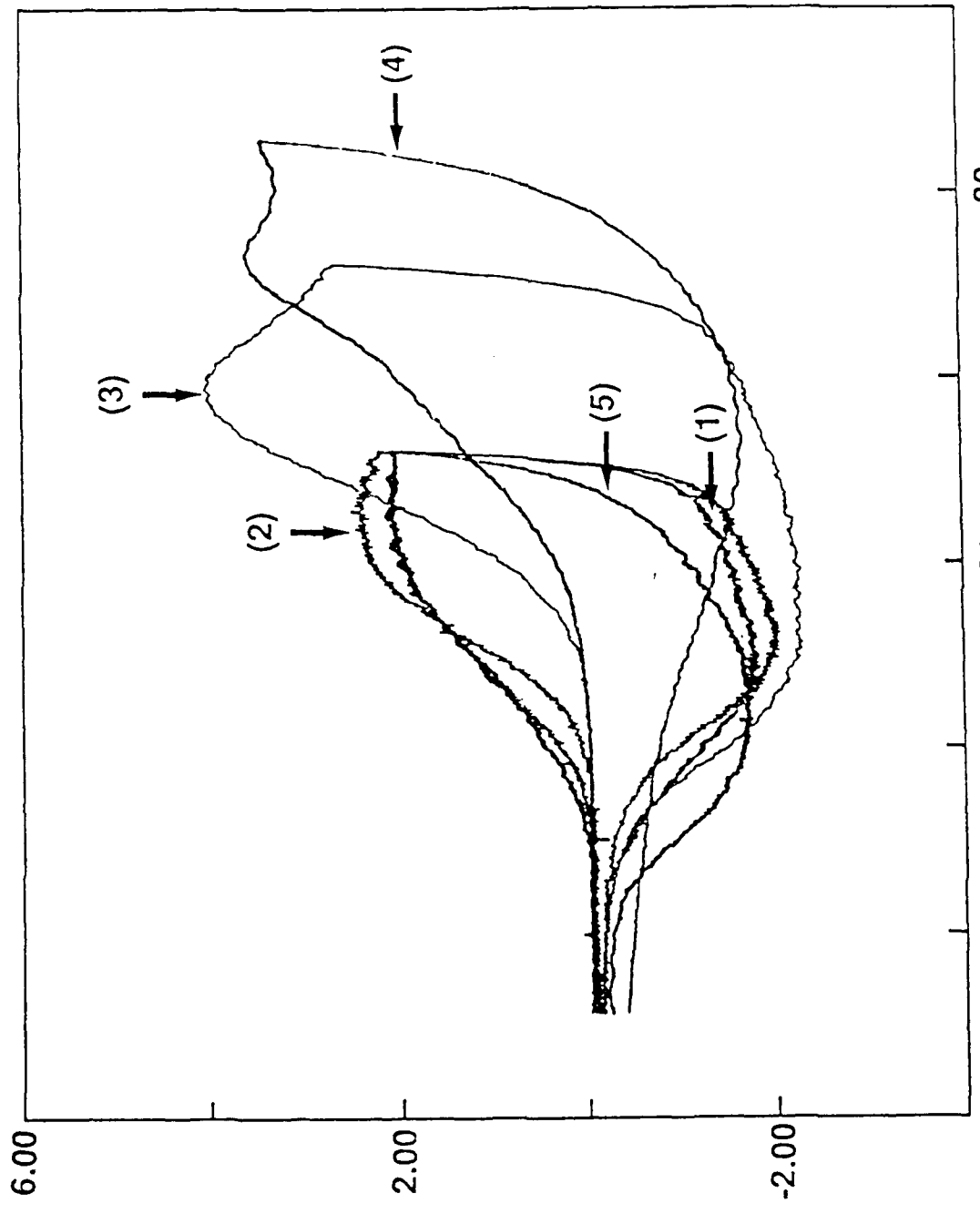
Current x10⁴, amps
6.00
2.00
-2.00
-.90
-.30
.30
E, volts vs. Ag/AgCl
(1)
(2)
(3)
(4)
(5)

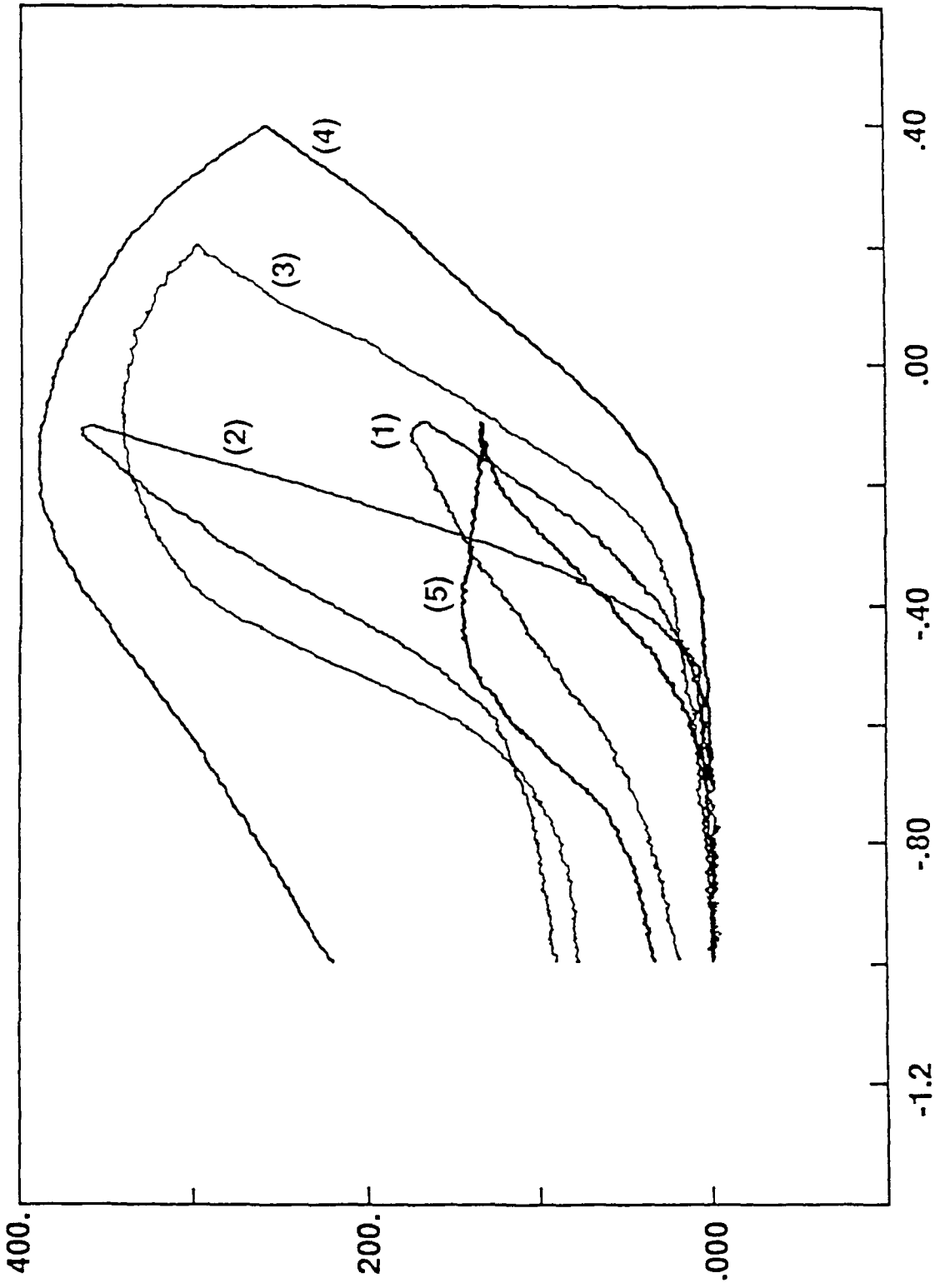
Frequency Change,Hz
400.
200.
.000
-1.2
-.80
-.40
.00
.40
E, volts vs. Ag/AgCl
(1)
(2)
(3)
(4)
(5)

F 5a

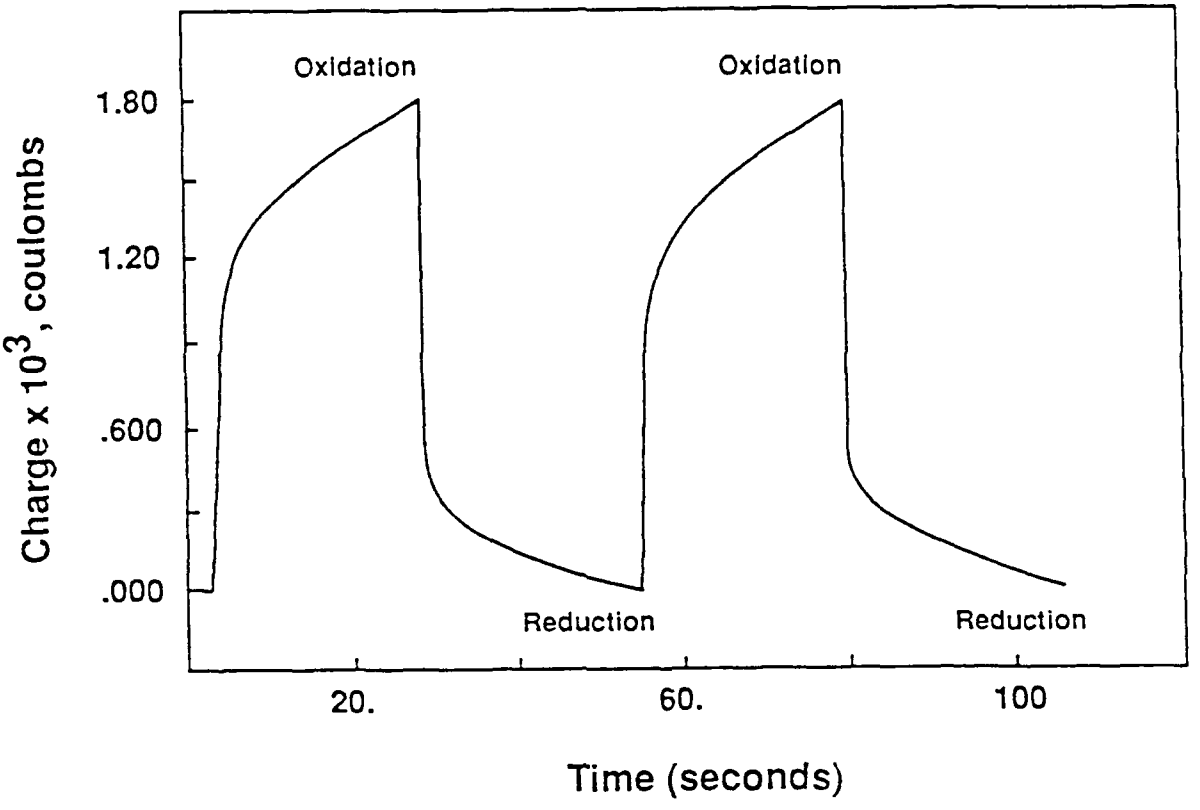
Oxidation
Oxidation
1.80
1.20
.600
.000
Charge x 10^3, coulombs
Reduction
Reduction
20.
60.
100
Time (seconds)

FSb

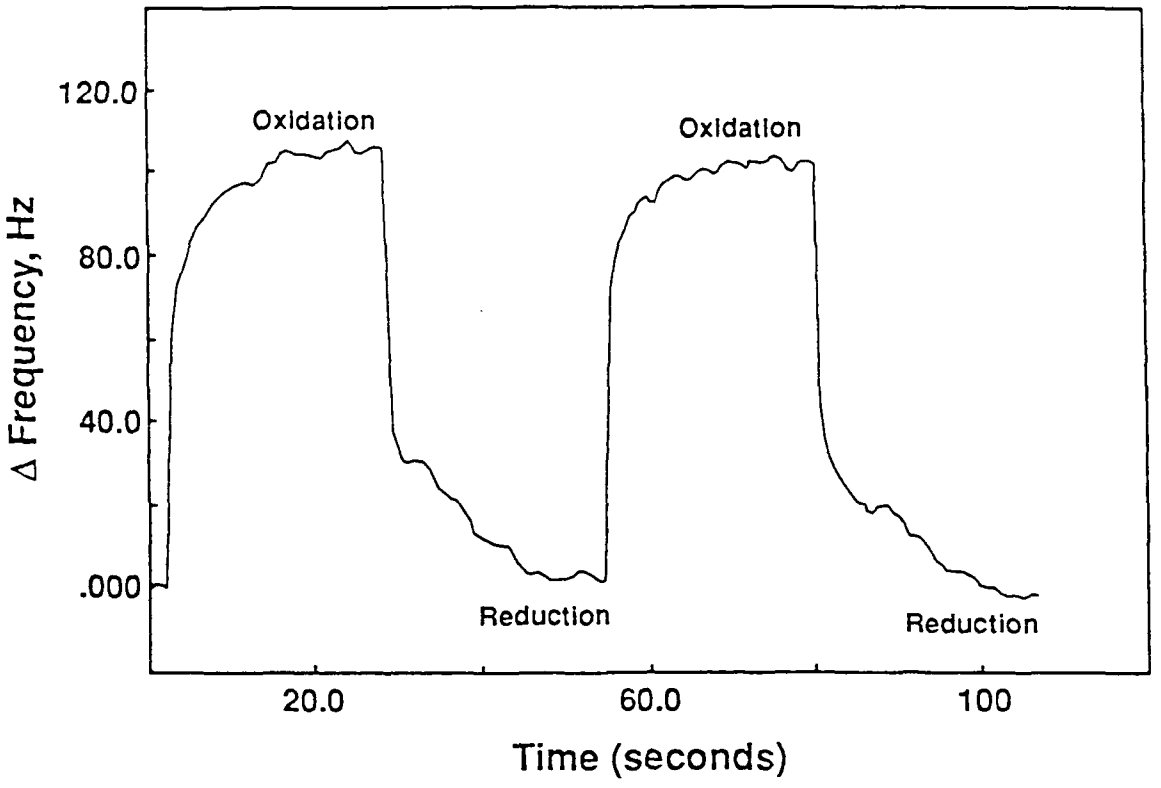
120.0
80.0
40.0
.000
Δ Frequency, Hz
Oxidation
Oxidation
Reduction
Reduction
20.0
60.0
100
Time (seconds)

F6

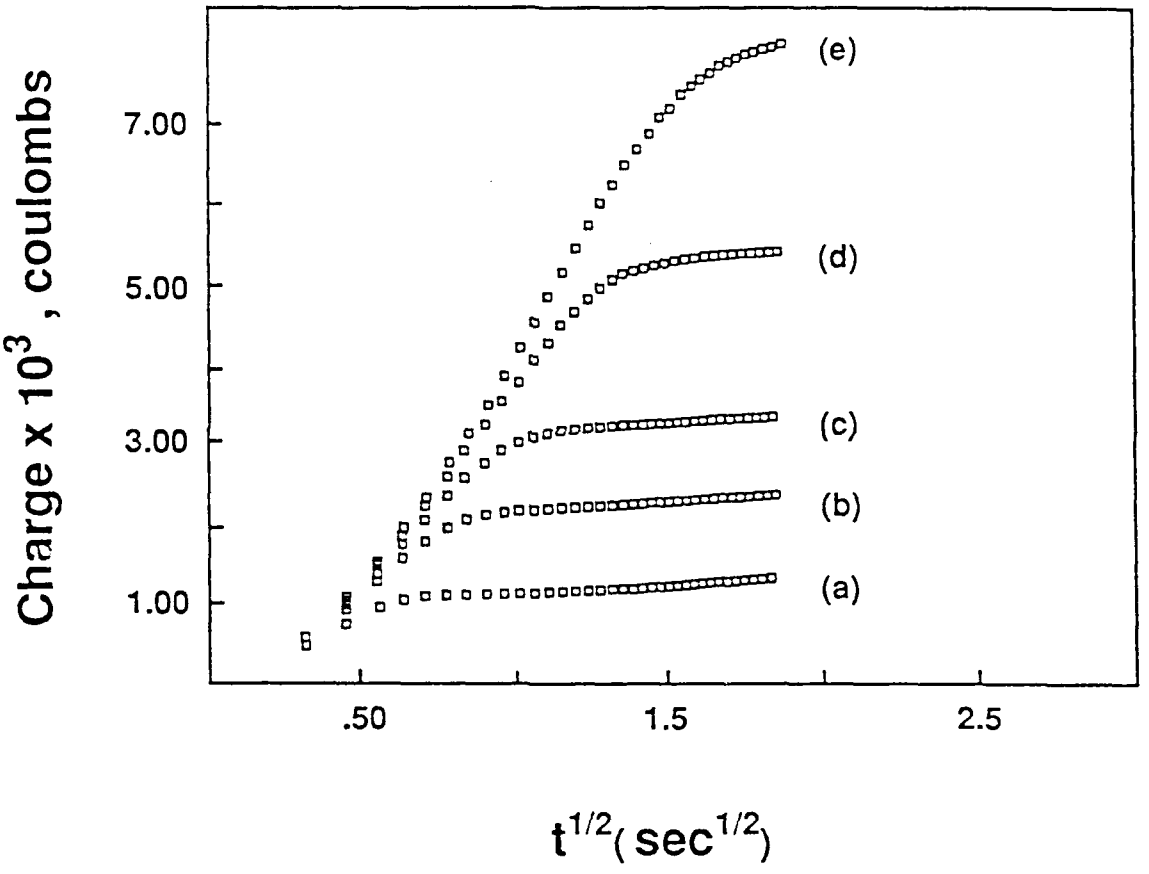

F7

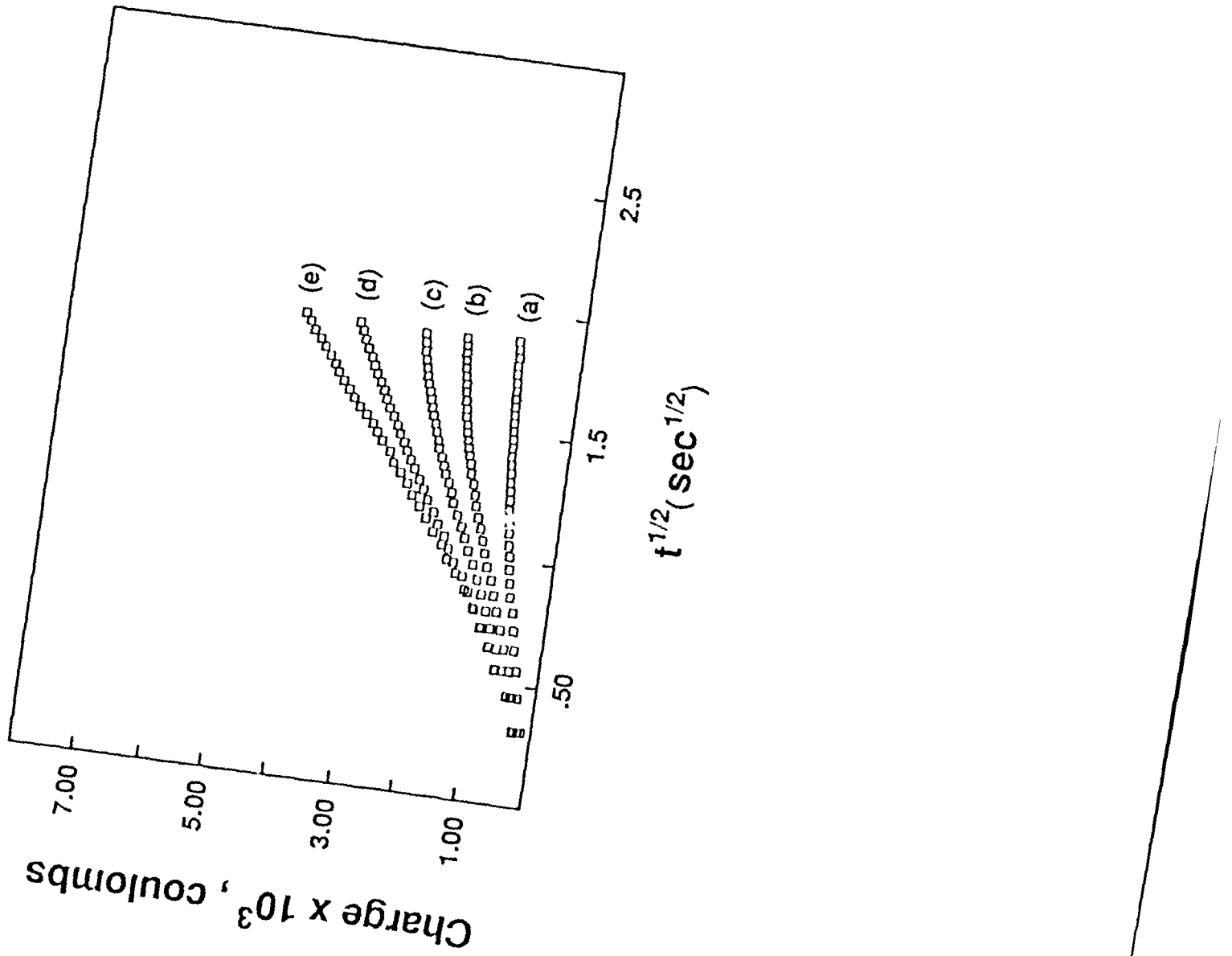

F 8

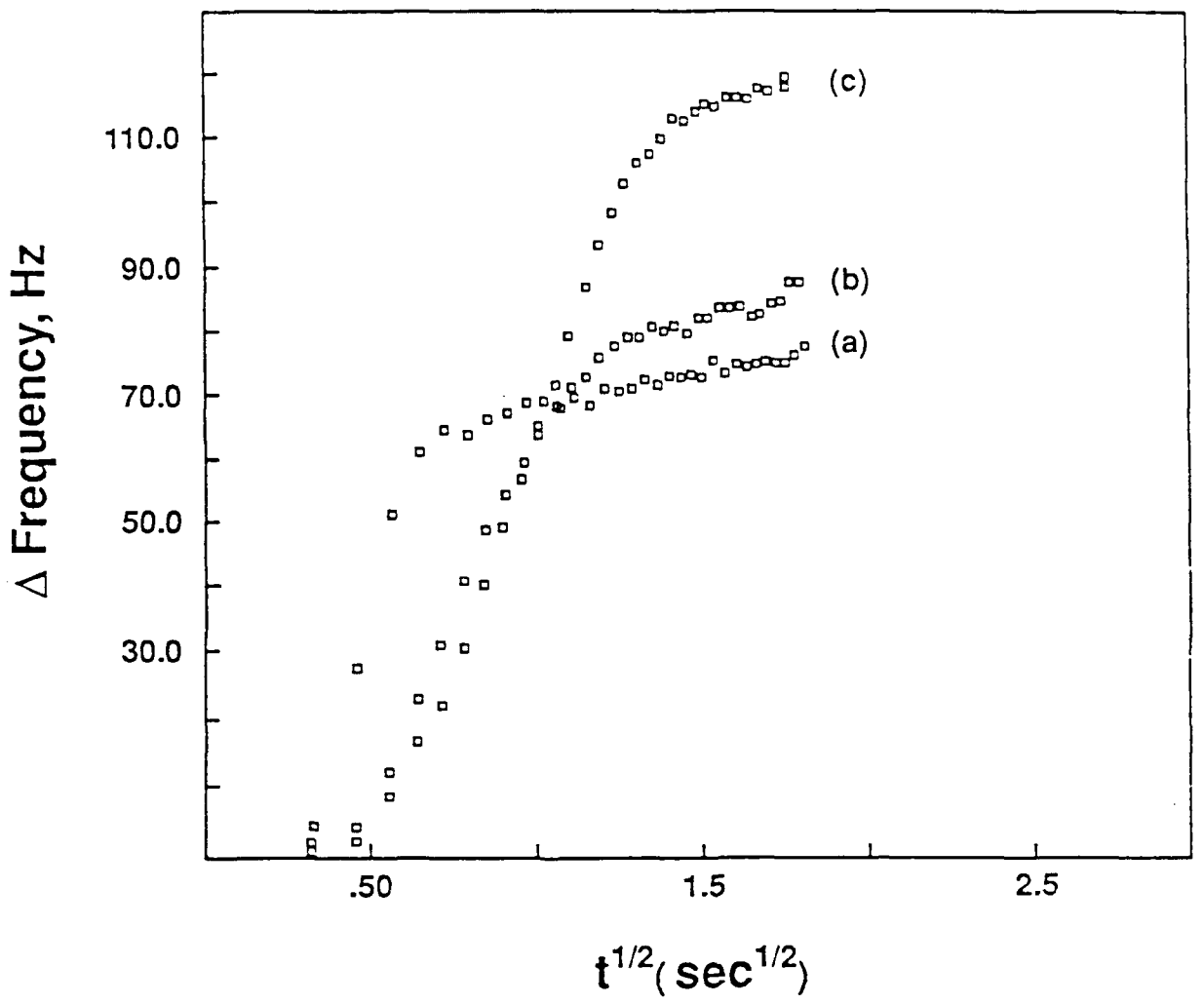

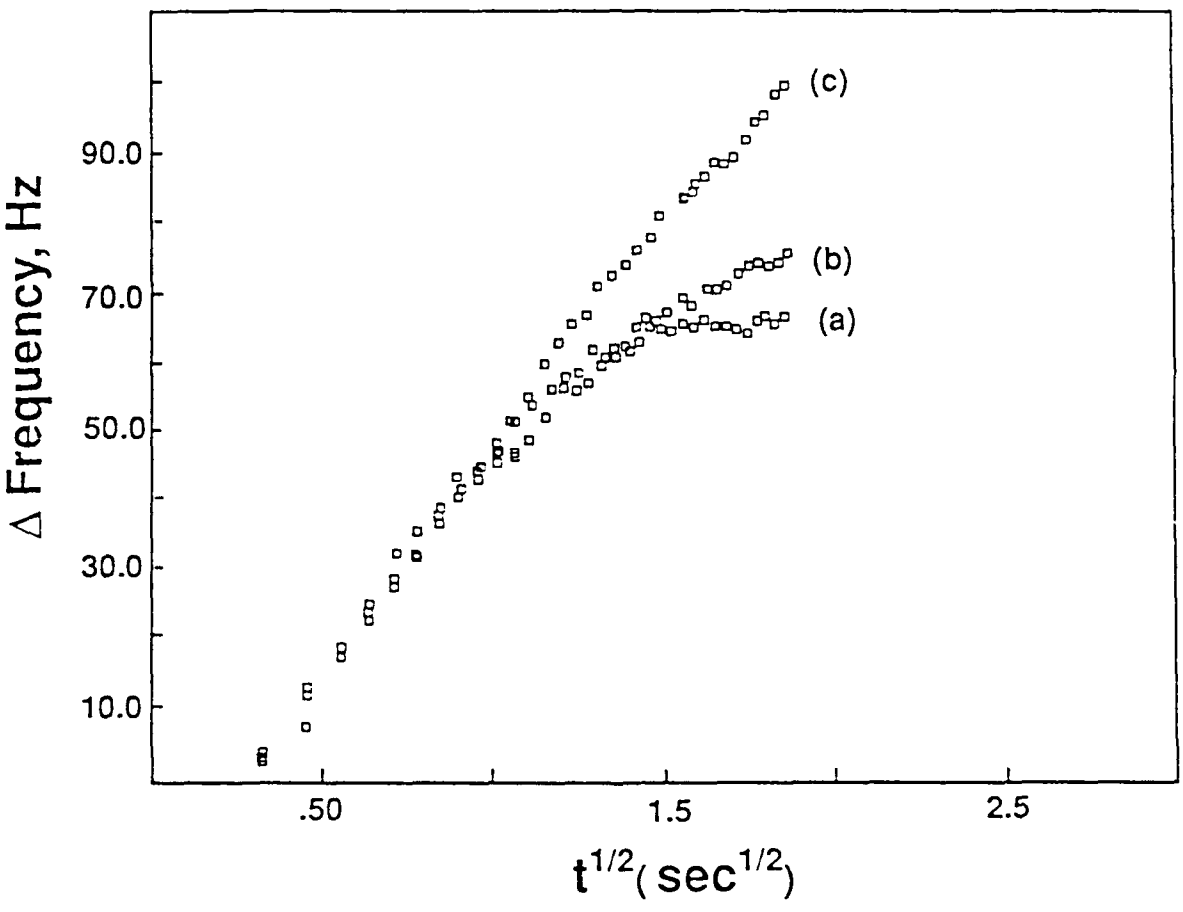
Δ Frequency, Hz
90.0
70.0
50.0
30.0
10.0
.50
1.5
2.5
t^1/2(sec^1/2)
(c)
(b)
(a)

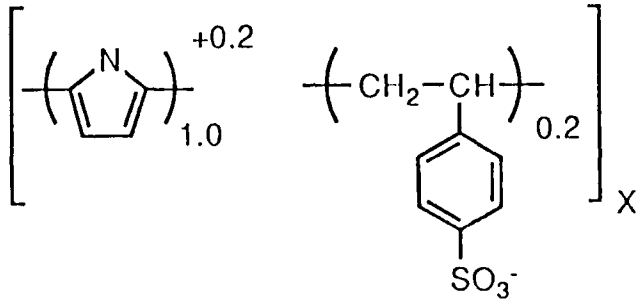

1